J Neurophysiol 103: 2002–2014, 2010.
First published January 27, 2010; doi:10.1152/jn.01038.2009.

Singing-Related Neural Activity Distinguishes Four Classes of Putative Striatal Neurons in the Songbird Basal Ganglia

Jesse H. Goldberg and Michale S. Fee

McGovern Institute for Brain Research, Department of Brain and Cognitive Sciences, Massachusetts Institute of Technology, Cambridge, Massachusetts

Submitted 25 November 2009; accepted in final form 26 January 2010

Goldberg JH, Fee MS. Singing-related neural activity distinguishes four classes of putative striatal neurons in the songbird basal ganglia. *J Neurophysiol* 103: 2002–2014, 2010. First published January 27, 2010; doi:10.1152/jn.01038.2009. The striatum—the primary input nucleus of the basal ganglia—plays a major role in motor control and learning. Four main classes of striatal neuron are thought to be essential for normal striatal function: medium spiny neurons, fast-spiking interneurons, cholinergic tonically active neurons, and low-threshold spiking interneurons. However, the nature of the interaction of these neurons during behavior is poorly understood. The songbird area X is a specialized striato-pallidal basal ganglia nucleus that contains two pallidal cell types as well as the same four cell types found in the mammalian striatum. We recorded 185 single units in Area X of singing juvenile birds and, based on singing-related firing patterns and spike waveforms, find six distinct cell classes—two classes of putative pallidal neuron that exhibited a high spontaneous firing rate (>60 Hz), and four cell classes that exhibited low spontaneous firing rates characteristic of striatal neurons. In this study, we examine in detail the four putative striatal cell classes. Type-1 neurons were the most frequently encountered and exhibited sparse temporally precise singing-related activity. Type-2 neurons were distinguished by their narrow spike waveforms and exhibited brief, high-frequency bursts during singing. Type-3 neurons were tonically active and did not burst, whereas type-4 neurons were inactive outside of singing and during singing generated long high-frequency bursts that could reach firing rates over 1 kHz. Based on comparison to the mammalian literature, we suggest that these four putative striatal cell classes correspond, respectively, to the medium spiny neurons, fast-spiking interneurons, tonically active neurons, and low-threshold spiking interneurons that are known to reside in area X.

INTRODUCTION

The striatum is the main input nucleus of the basal ganglia (BG) circuit and is widely implicated in motor control and learning (Graybiel 2008). Inactivations or lesions of the striatum result in impaired motor learning while neuropsychiatric disorders such as obsessive compulsive disorder and Huntington's diseases are associated with striatal dysfunction (Packard and Knowlton 2002). For decades, striatal function has been interpreted mainly in terms of the relatively large population of GABAergic medium spiny neurons (MSNs) that constitute striatal outputs (Hikosaka and Wurtz 1989). However, several interneuronal subtypes within the striatum are increasingly considered key components of BG function. Specifically, anatomical, histological, and physiological studies in brain slices indicate that the striatum contains at least four cell classes—MSNs, as well as three classes of striatal interneuron: fast-spiking interneurons, tonically active cholinergic neurons, and low-threshold spiking interneurons (Kreitzer 2009). Surprisingly, the neural activity of all of these cell classes has not been described during a single behavior.

MSNs, the striatal output neurons, are the most numerous cell class (Wilson and Groves 1981). In brain slices, they are distinguished by their densely spiny dendritic arbor and their expression of the neuropeptides substance P or enkephalin (Mink 1996). During behavior, MSNs are distinguished by their low firing rates and their sparse neural activity that is often precisely time-locked to specific events and movements in a behavioral sequence (Barnes et al. 2005; Hikosaka and Wurtz 1989; Jin et al. 2009).

Fast-spiking interneurons (FS) are distinguished in brain slices by their high-frequency firing and their expression of the calcium-binding protein parvalbumin and of KV3-type potassium channels, which contribute to their uniquely narrow spike waveforms (Kubota et al. 1993; Lenz et al. 1994; Plenz and Kitai 1998). In vivo juxtacellular recording and labeling of FS neurons has confirmed that they are distinguishable by their narrow spike waveforms (Mallet et al. 2005), and this criterion has recently been used in the first study to characterize their activity during behavior. In contrast to MSNs, FS neurons exhibited constant firing (~20 Hz) and weak correlation to events in a well-learned maze task (Berke 2008).

Tonically active neurons (TANs), the cholinergic neurons of the striatum, are distinguished morphologically by their large cell bodies and expansive aspiny dendritic arbors (Zhou et al. 2002). Intracellular recording and labeling of TANs in vivo has demonstrated that they are distinguishable physiologically by their tonic activity and their long afterhyperpolarizations (Wilson et al. 1990). During behavior, TANs, in contrast to FS and MSN neurons (Berke 2008), do not generate high-frequency bursts and instead fire tonically at rates that can be modulated by a variety of events within a behavioral task, including reward, movement, and sensory stimuli (Aosaki et al. 1995; Apicella 2007; Morris et al. 2004).

Finally, perhaps the least understood of the striatal cell classes is the low-threshold spiking (LTS) interneuron. In brain slice studies, LTS neurons exhibit rebound low-threshold calcium bursts after release from hyperpolarization (Kubota and Kawaguchi 2000). To our knowledge, there are no reported recordings of LTS neurons in the behaving animal, although under anesthesia, putative LTS neurons reach the highest peak rate of all striatal neurons and discharge primarily in long bursts that contain multiple spikes (Sharott et al. 2009).

The goal of the present study was to record from all four of these striatal cell types during a BG-dependent behavior. To this end, the songbird presents an ideal model system. Songbirds have a specialized BG thalamocortical circuit, called the anterior fore-

Address for reprint requests and other correspondence: M. S. Fee, McGovern Institute for Brain Research, Massachusetts Institute of Technology, MIT 46-5133, 77 Massachusetts Ave., Cambridge, MA 02139 (E-mail: fee@mit.edu).

brain pathway (AFP; Fig. 1*A*), that is required for song learning (Nottebohm et al. 1976; Scharff and Nottebohm 1991). Area X, the input nucleus of the AFP, contains the same four striatal cell classes that are found in the mammalian striatum (Fig. 1*B*) (Farries and Perkel 2002) as well as two pallidal cell classes that, as in mammals, can be distinguished from striatal cell types on the basis of their high spontaneous firing rate (DeLong 1972; Farries and Perkel 2002; Farries et al. 2005). The strong homology between the songbird and mammalian BG (Fig. 1*B*) is consistent with mounting evidence that the BG microcircuit has been conserved for >300 million years and predates the division of birds, mammals, and reptiles into separate classes (Reiner 2009).

We have recorded single neurons in area X of singing juvenile birds. Based on spike waveforms and singing-related neural activity, we find six distinct cell classes. In this study, we focus on the four cell classes that exhibited the low spontaneous firing rates (<30 Hz) that distinguish striatal from pallidal cell types (DeLong 1972; Johnstone and Rolls 1990). Notably, we find that the four putative striatal cell classes in the songbird area X exhibit singing-related firing patterns similar to the neural activities exhibited by their possible mammalian homologues: MSNs, FS interneurons, TANs and LTS interneurons. In addition, just as mammalian striatal neurons are correlated with the timing of ongoing behavioral tasks, all area X neurons exhibited significant correlations with the timing of specific syllables.

Our results provide a framework for the classification of extracellularly recorded striatal neurons in the songbird and include the first characterization of the singing-related neural activities of multiple cell types in a BG nucleus required for song learning.

METHODS

Animals

Subjects were 21 juvenile male zebra finches, 40–70 days post hatch (dph). Birds were obtained from the MIT zebra finch breeding

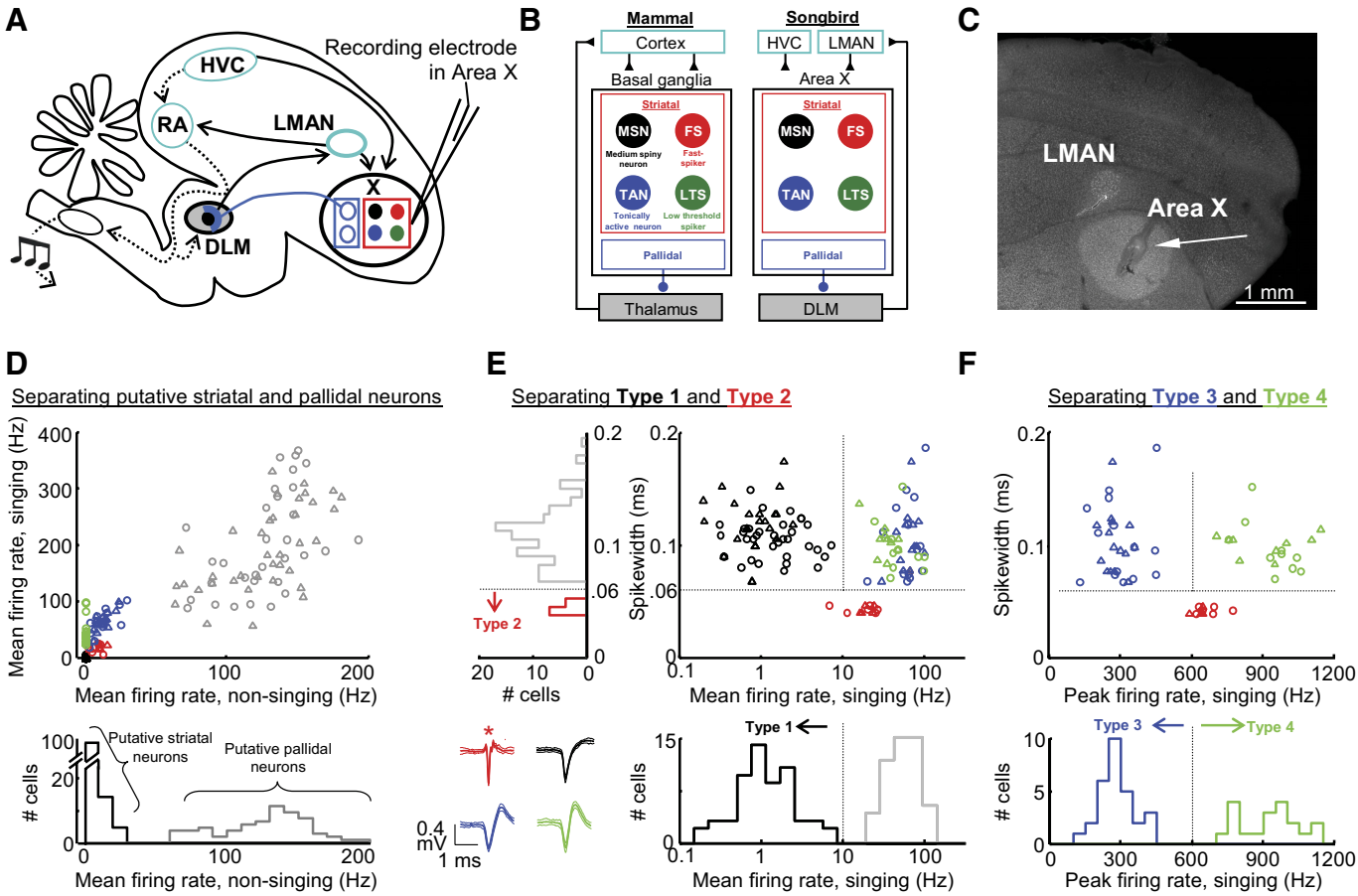

FIG. 1. Singing-related neural activity distinguishes four classes of putative striatal neurons in area X. *A*: schematic of the avian song circuit showing the anterior forebrain pathway (AFP, —) containing the basal ganglia structure area X, and the motor pathway (···). *B*: the songbird area X is a striato-pallidal structure that resides in a thalamo-cortical loop. Four cell classes found in the mammalian striatum are also found in area X: medium spiny neurons, fast spiking interneurons (FS), tonically active neurons (TANs), and low-threshold spiking interneurons (LTS). *C*: representative histology for area X recordings. Small electrolytic lesions were made with the recording electrodes (←) to verify electrode position within area X. *D, top*: the mean firing rate during singing is plotted against the mean firing rate during nonsinging epochs for all neurons recorded in Area X. *Bottom*: histogram of nonsinging firing rates separates 2 classes of neurons: putative pallidal neurons that fired at high rates (>50 Hz), and putative striatal neurons that fired at low rates (<30 Hz). *E*: for all putative striatal neurons, the spike width is plotted against the mean firing rate during singing. The bottom histogram distinguishes type-1 neurons, which fired at low rates during singing (<10 Hz). *Left*: histogram distinguishes type-2 neurons, which had thin spike widths (<0.06 ms, see METHODS). *Inset*: spike waveforms (means ± SD, $n = 50$ spikes) from representative neurons of each cell class. *, thin spike of a type-2 neuron. *F*: for all putative striatal neurons (excluding type-1), the spikewidth is plotted against the peak firing rate during singing (99th percentile rate, see METHODS). Histogram of peak firing rate distinguishes an additional 2 classes of neurons: type-3 neurons that do not generate high-frequency discharge (peak rate: <600 Hz), and type-4 neurons that do (peak rate: >600 Hz). For all scatter plots, △ and ○, neurons recorded from subsong and plastic song birds, respectively.

facility (Cambridge, MA). The care and experimental manipulation of the animals were carried out in accordance with guidelines of the National Institutes of Health and were reviewed and approved by the MIT Committee on Animal Care. All data are from juvenile birds singing undirected song.

Chronic neural recordings and histology

Recordings were carried out using a motorized microdrive described previously (Fee and Leonardo 2001). Units accepted for analysis had signal-to-noise ratios (average spike peak amplitude compared with SD of noise) >10:1. Data were acquired and analyzed using custom Matlab software (A. Andalman, D. Aronov and J. H. Goldberg). Small electrolytic lesions (20 μA for 15 s) were made through the electrodes at the conclusion of experiments for histological verification of electrode position.

Data analysis

Spikes were sorted off-line using custom Matlab software. We represented neural activities as instantaneous firing rates, $R(t)$, defined at each time point as the inverse of the enclosed interspike interval (ISI) as follows (*Eq. 1*)

$$R(t) = \frac{1}{t_{i+1} - t_i}, \quad \text{for} \quad t_i < t \leq t_{i+1}$$

where t_i is the time of the ith spike. Peak firing rates (99th percentile rate) were calculated for each neuron as the inverse of its first percentile ISI. All ISI distributions were computed in bins that were evenly spaced in log time. Interbout periods were defined as silent periods separated from singing by <5 s. Note that the interbout periods include the silent periods immediately preceding bout onset as well as following bout offset. Nonsinging firing rates were calculated from spiking activity during silent periods separated by singing by >10 s. We used song to automatically trigger data acquisition as well as manually recorded tens of seconds of data periodically during nonsinging periods. We did not acquire data continuously during nonsinging periods. Thus the anecdotal observation that bursting in type-4 neurons may precede the onset of singing by tens of seconds is not supported by a quantitative analysis but is based on the recollection of the experimenters listening to neuronal activity on the audio monitor (Grass AM10).

Burst definition

While the classification of the four cell types did not depend on any definition of burst, we included a burst analysis to highlight differences in firing patterns that were not explicitly part of their classification scheme. Bursts were defined as a simple threshold-crossing of 250 Hz in the instantaneous firing rate (IFR). This threshold was based on the ISI distributions of the four cell classes—specifically that neurons types 1, 2, and 4 had peaks in their ISI distributions <4 ms, whereas type-3 neurons did not (Fig. 7*A*). The observation that type-3 neurons did not burst was consistent with their relatively flat spike train autocorrelation functions (Fig. 7*C*).

Spike width identification of type-2 neurons

For each neuron, the spike width was calculated as the half-width of the negative going deflection of the average of 50 spike waveform examples, resulting in a total of 115 spike widths (115 neurons). The spike widths of type-2 neurons lay in a distinct cluster of 11 neurons separated by a gap 0.021 ms to the left of the edge of the remaining distribution. To determine the likelihood that such a distinct cluster could emerge from an underlying Gaussian distribution, we performed a Monte Carlo analysis where we generated 10,000 surrogate datasets of 115 spike widths, each drawn from a single Gaussian distribution with the same mean and SD as the observed dataset. From the surrogate datasets, we determined the probability of finding ≥11 samples to the left of a gap of ≥0.02 ms. We found that in 0/10,000 datasets did such a condition exist. In fact, we found that even the observation of five samples to the left of a gap of 0.01 ms was extremely rare ($P = 0.02$).

Analysis of correlations of neural activity to song temporal structure

For plastic song birds, syllables were identified both manually and with an automated clustering algorithm (A. Andalman) that uses standard acoustic features of zebra finch song (Tchernichovski et al. 2000). The songs of the plastic song birds in this study were not yet organized into motifs—thus we analyzed correlations on a syllable-by-syllable basis. We included in this analysis only those birds with song repertoires that included distinct, identifiable syllables and only analyzed cells that were recorded for >30 syllable renditions (mean number of syllables per neuron = 169, range: 31–2,053). Neural activity from 60 ms prior to syllable onsets to 60 ms following the median syllable duration was linearly time-warped, using as a reference the syllable's median duration as described previously (Kao et al. 2008; Ölveczky et al. 2005). Syllables of subsong birds (<50 dph) are highly unstructured, and neural correlations to their acoustic or temporal structure are outside the scope of this study.

To determine the significance of firing rate peaks and minima within syllables, a rate histogram (10-ms bin size) was generated of the syllable-aligned spike trains. Surrogate histograms were also calculated for all spike trains after a random time shift as described previously (Ölveczky et al. 2005). The shift was circular, such that spikes wrapped around to the beginning of the spike train. For each cell, the correlation distribution of the time-shifted firing rates was calculated with 1,000 different ensembles of random shifts. Peaks and minima in firing rate were considered significant when they crossed the 1st (for minima) and 99th (for peaks) percentile of the compiled minima and maxima of the surrogate histograms.

Quantification of sparseness

A "sparse" firing distribution of a neuron is one in which it gives a weak response during most stimuli (or movements), but a strong response during one stimulus (or movement) (Field 1994; Hahnloser et al. 2002). We used an "entropy" measure of sparseness (Lehky et al. 2005; Tolhurst et al. 2009) to quantify how selective neuronal activity was for specific times in the song. For each neuron, we calculated syllable-aligned rate histograms for every syllable (10-ms bin size as described in the preceding text), resulting in a total of N bins. These histograms were normalized over all syllables to generate a time-varying probability spike density function, p_i, where the ith value indicated the normalized firing probability of that neuron within that time bin. Thus the sum of all points in this vector of length N was equal to 1 ($\sum_i^N p_i = 1$). We then computed an entropy based sparseness index (Lehky et al. 2005) as follows (*Eq. 2*)

$$\text{Sparseness\_Index} = 1 + \frac{\sum_{i=1}^{N} p_i \log(p_i)}{\log(N)}$$

The sparseness index is equal to 1 (maximal sparseness) when activity is restricted to a single portion of the song (a single 10-ms bin) and goes to zero when spikes are evenly distributed throughout the song.

Trial-to-trial correlation analysis

To quantify trial-to-trial differences in neural activity on short time scales, we computed the correlation coefficient (CC) between the instantaneous firing rate for all sets of trials, as follows (*Eqs. 3* and *4*),

$$CC = \frac{1}{N_{\text{pairs}}} \sum_{j>i}^{N_{trials}} \text{CC}_{ij}$$

$$CC_{ij} = \frac{\langle \hat{r}_i(t)\hat{r}_j(t)\rangle_t}{\sqrt{\langle \hat{r}_i(t)^2\rangle_t \langle \hat{r}_j(t)^2\rangle_t}}$$

where $\hat{r}(t)$ is the mean-subtracted spike train smoothed with a Gaussian kernel of 20 ms SD (Kao et al. 2008; Ölveczky et al. 2005). To determine the statistical significance of the correlation, we also compared the correlation distributions to those calculated after random, circular time shifts were added to the spike trains, as described in the preceding text, and considered as significant those correlations where the correlation distribution was significantly different from that of the randomly shuffled spike trains ($P < 0.01$, Kolmogorov-Smirnov test). Finally, we also calculated CCs on non time-warped syllables, resulting in, on average a 0.01 decrease in CC value. To aid in interpreting the meaning of the CC values, here we report the values of the CCs for each neuron whose activity is shown in a figure with a raster plot: Fig. 2*B*: 0.41; Fig. 4*F*: 0.018 and 0.035 (syllables "a" and "b"); Fig. 5*F*: 0.11 and 0.061 (syllables "a" and "b"); Fig. 6*F*: 0.041, 0.079, and 0.035 (syllables "a," "b," and "c").

RESULTS

Nonsinging firing rate distinguishes putative pallidal and striatal neurons in area X

We recorded 185 neurons in area X of 10 juvenile birds, aged 40–70 dph (see METHODS). In awake, nonsinging birds, we found that the average firing rate of area X neurons fell into two main classes: high-frequency (HF) neurons with average nonsinging firing rates >60 Hz (127 ± 30 Hz, $n = 70$, all error bars indicate SD unless otherwise stated), and low-frequency neurons with average nonsinging rates <30 Hz (4.9 ± 6.3 Hz, $n = 115$; Fig. 1*D*). We hypothesize that the high and low firing cell classes represent the pallidal and striatal neuronal cell classes, respectively, that are known to reside in area X (Farries and Perkel 2002). This hypothesis is based on previous studies of area X neurons in brain slices, which revealed high spontaneous firing rates in pallidal neurons and low rates in striatal neurons (Farries and Perkel 2002), and in vivo, which found that HF neurons in area X project to DLM (Leblois et al. 2009), as well as on numerous reports in mammals demonstrating high pallidal and low striatal firing rates in awake animals (Bar-Gad et al. 2003; DeLong 1972; Johnstone and Rolls 1990), In the present study, we focus exclusively on the putative striatal neurons.

Singing-related neural activity distinguishes four classes of putative striatal neuron in area X

Three measures of the neural activity divided the putative striatal neurons into four distinct classes: spike width, mean firing rate during singing, and peak firing rate (99th percentile rate, see METHODS) during singing. We first plotted spike width versus mean firing rate during singing and observed three distinct clusters. Type-1 neurons were defined by a firing rate <10 Hz and a spike width >0.06 ms (Fig. 1*E*, black cluster, $n = 56$). Type-2 neurons formed a distinct cluster of narrow spike waveforms (<0.06 ms; Fig. 1*E*, red cluster, $n = 11$, $P < 0.0001$, see METHODS). A third cluster had high mean firing rates during singing (>10 Hz) and broad spike waveforms (>0.06 ms; Fig. 1*E*, blue and green data points). Neurons within this cluster were bisected by their peak firing rates during singing (99th percentile rate, see METHODS)—type-3 neurons (Fig. 1*F*, blue cluster, $n = 29$) did not generate high-frequency bursts, exhibiting peak rates <600 Hz, while type-4 neurons (green cluster, $n = 19$) generated bursts at rates >600 Hz and frequently discharged at peak rates exceeding 1 kHz. We now consider the properties of each of these cell classes in turn.

Type-1 neurons exhibit sparse, temporally precise discharge during singing

A defining feature of type-1 neurons was their low average firing rate (Fig. 2). During nonsinging periods, type-1 neurons did not spike (<0.01 Hz, $n = 56/56$ neurons). During singing, spikes occurred more frequently (average rate = 1.58 ± 1.46 Hz), and occasionally discharged in brief bursts (Fig. 2, *A* and *B*). We defined bursts as events exceeding 250 Hz (see METHODS) and found that all type-1 neurons generated bursts that could reach high rates (peak firing rate within bursts = 480 ± 187 Hz; burst/s = 0.15 ± 0.12 s^{-1}, $n = 56$ neurons). The mean and peak firing rates exhibited by type-1 neurons during singing or nonsinging did not differ between subsong and plastic song birds (Table 1, $P > 0.05$, unpaired *t*-test, $n = 22$ and $n = 34$ neurons from subsong and plastic song birds, respectively).

In plastic song birds, where specific syllables could be identified (see METHODS), type-1 neurons exhibited sparse activity that was precisely locked to the occurrence of particular syllables or even specific times within single syllables (Fig. 2, *A* and *B*). We analyzed how neural activity was correlated with song timing in three ways. First, to quantify how spiking was distributed across the song, for each neuron, we computed an entropy-based sparseness index where a value of 1 indicated a neuron whose activity was entirely restricted to one portion of the song and a value of zero indicated a neuron that spiked evenly across the song (see METHODS). The activity of type-1 neurons was significantly more sparse than all other area X neurons (Fig. 2*C*, Table 1, sparseness index: type-1 = 0.45 ± 0.14, $n = 31$; types-2 to -4 = 0.023 ± 0.018, $n = 25$, $P < 0.0001$ unpaired *t*-test).

Second, to quantify the trial-to-trial variability in the firing rate modulations across multiple syllable renditions, we computed pairwise correlation coefficients (CCs) between smoothed spike trains of different song renditions (see METHODS). In all type-1 neurons recorded in plastic song birds, the timing of spikes was reproducible across repeated syllable renditions (CC = 0.26 ± 0.22, range: 0.02–0.85, $n = 44$ syllables from 31 neurons). We note, however, that even when neuronal activity was precisely time-locked to a given syllable, the number of spikes discharged was variable (Fig. 2*E*). On average, neurons spiked during less than half of the renditions of the syllable during which they spiked most reliably (39 ± 25%, range: 4.7–100%; Fig. 2*E*).

Third, to determine how neural activity was distributed within individual syllables, for each neuron we computed syllable-aligned rate histograms (as in Fig. 2*B*, *bottom*) and examined the temporal location of significant rate peaks (see METHODS). As a group, different type-1 neurons tended to spike at different times in the song (Fig. 2*D*) and at different times within syllables. Significant rate peaks were uniformly distrib-

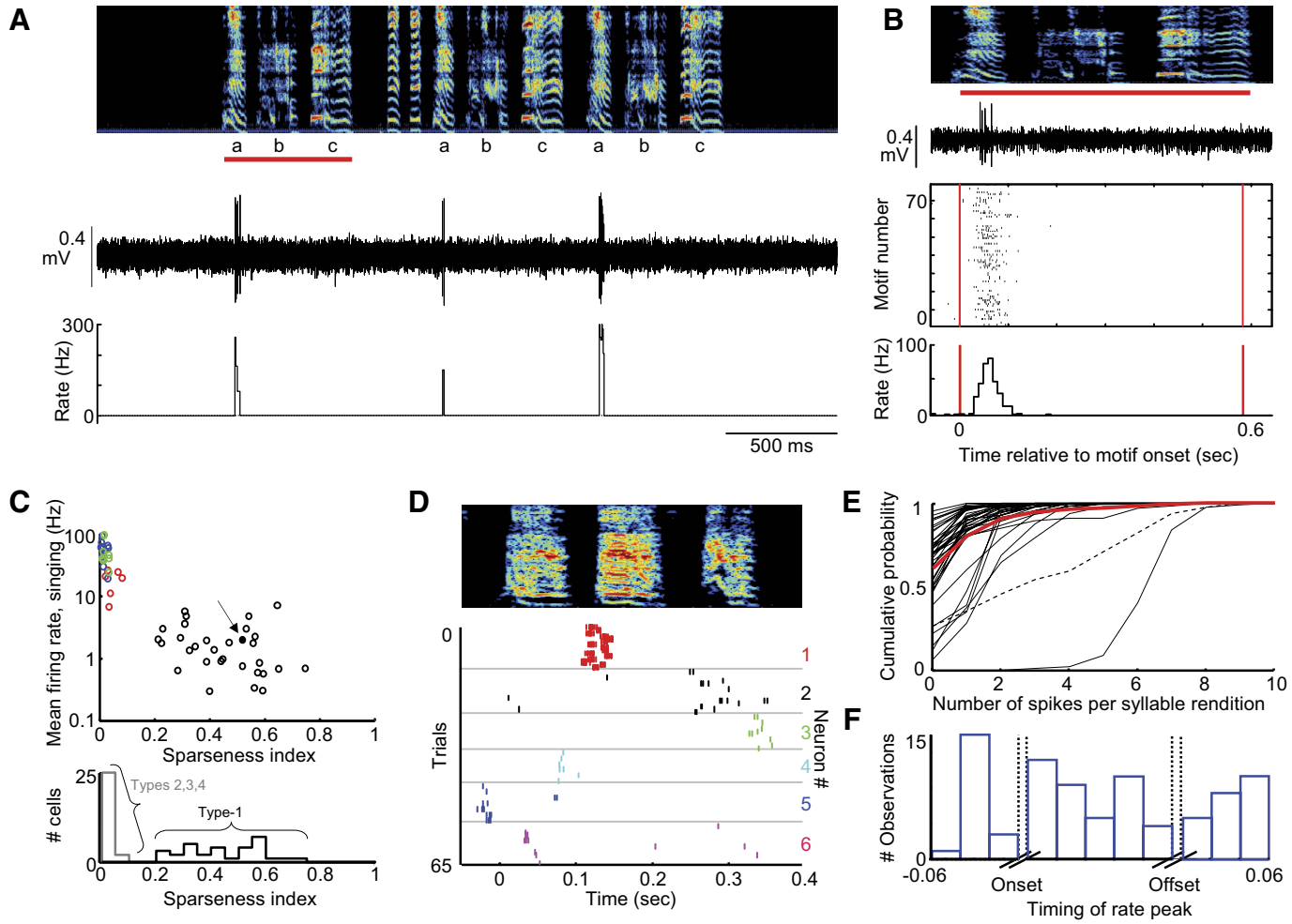

FIG. 2. Type-1 neurons exhibit sparse, temporally precise singing-related activity. *A*: the raw voltage trace of a type-1 neuron and its instantaneous firing rate (see METHODS) are plotted beneath the spectrogram (age 64 dph). Note that this neuron spikes only during syllable "a" of a 3-syllable motif. *B, top*: expanded view of the voltage and spectrogram from the 1st motif from *B* (indicated by red bar). *Middle*: spike raster indicating spiking activity of this neuron during 73 renditions of the motif. *Bottom*: rate histogram compiled from the raster plot. *C, top*: for each putative striatal neuron recorded in a plastic song bird, the mean firing rate during singing is plotted against the sparseness index; color code as in Fig. 1 (see METHODS). The neuron from *A* and *B* is labeled with a solid black dot and an arrow. *Bottom*: histogram of sparseness index. *D*: spectrogram and spike raster of 6 type-1 neurons recorded in one bird (different bird from *A* and *B*) during ages 61–65 days post hatch (dph). Each neuron exhibits sparse activity temporally localized to distinct parts of a 3-syllable motif. *E*: cumulative probability plots of the number of spikes generated per syllable for all type-1 neurons recorded in plastic song birds. Red trace represents the average of 44 syllables from 31 neurons, and the dashed trace is from the neuron in *A* and *B*. Syllables that never contained a spike were excluded from this analysis. *F*: population histogram showing the distribution of significant rate peaks as a function of syllable timing. Data were compiled from 44 syllables from 31 type-1 neurons. Note that significant peaks occur throughout the syllables.

uted within syllables with no preferential correlation to the onset or offset of syllables (Fig. 2*F*, see METHODS).

Finally, some type-1 neurons ($n = 9$) discharged in precise relation to the onset or offset of song bouts as has been observed in many lateral magnocellular nucleus of the anterior nidopallium (LMAN) neurons that project to area X (Fig. 3; $n = 4$ and $n = 5$ in subsong and plastic song aged birds, respectively) (Aronov et al. 2008).

Thin-spiking, type-2 neurons exhibit brief high-frequency bursts throughout the song

Type-2 neurons were distinguished by their narrow spike waveforms (Fig. 1*E*). In contrast to type-1 neurons, type-2 neurons exhibited steady, low-frequency firing during nonsinging (7.9 ± 4.4 Hz, $n = 11/11$ neurons, Figs. 1*D* and 4*A*) with modest coefficient of variability in the duration of ISIs (CV_{ISI} = 1.36 ± 0.60; Fig. 4, *B* and *C*, Table 1). During singing, type-2 neurons exhibited higher firing rates and larger rate fluctuations (singing: mean rate = 19.1 ± 6.0 Hz, CV_{ISI} = 1.80 ± 0.37; $P < 0.001$ compared with nonsinging), including brief, high-frequency bursts (peak rate = 654 ± 51 Hz; burst/s = 2.27 ± 1.21 s^{-1}; Figs. 1, *D* and *E*, and 4, *A–C*). Bursting also occurred in the seconds immediately before and after song bouts (inter-bout silence, see METHODS) and was associated with a shift in the ISI distributions toward short intervals during singing and with a peak in the spike train autocorrelations at short times (Fig. 4, *B* and *C*). The firing patterns of type-2 neurons were indistinguishable in subsong and plastic song birds (Table 1, Fig. 4, $n = 5$ and 6 neurons from subsong and plastic song birds, respectively).

While type-1 neurons discharged sparsely at specific portions of the song, type-2 neurons discharged throughout the song (sparseness index = 0.044 ± 0.024) and exhibited sig-

TABLE 1. *Spiking statistics for area X cell classes in subsong and plastic song birds*

	Spikewidth, ms	Mean Rate, Singing, Hz	Mean Rate, Interbout, Hz	Peak Rate, Singing, Hz	Peak Rate, Interbout, Hz	% Spikes in Burst, Singing	# Of Spikes Per Burst, Singing	Correlation Coefficient	C.V.$_{ISI}$, Bout	C.V.$_{ISI}$, Interbout
Type-1, Subsong n = 22	0.12 ± 0.03	0.97 ± 0.58*	0.28 ± 0.36	437 ± 196	N.A.	25 ± 19	2.1 ± 0.2	N.A.	1.5 ± 0.4	N.A.
Type-1, Plastic n = 34	0.11 ± 0.02	1.98 ± 1.7*	0.32 ± 0.49	535 ± 267	N.A.	33 ± 25	2.6 ± 1.3	0.26 ± 0.22	1.7 ± .7	N.A.
Type-2, Subsong n = 5	0.043 ± 0.003	19.9 ± 3.6*	8.9 ± 2.3*	629 ± 27	714 ± 501	39 ± 14	3.2 ± 0.2	N.A.	1.8 ± 0.2	1.9 ± 0.7
Type-2, Plastic n = 6	0.044 ± 0.003	18.5 ± 7.8*	9.7 ± 4.2	672 ± 57	482 ± 134	31 ± 16	3.0 ± 0.4	0.017 ± 0.022	1.8 ± 0.4	1.6 ± 0.4
Type-3, Subsong n = 15	0.10 ± 0.03	65.6 ± 17.0*	20.8 ± 8.2	274 ± 45*	216 ± 71	4 ± 3	2.1 ± 0.1	N.A.	0.9 ± 0.1	1.5 ± 0.3
Type-3, Plastic n = 14	0.11 ± 0.04	64.6 ± 23.1*	18.7 ± 7.7	296 ± 102*	241 ± 136	8 ± 8	2.2 ± 0.2	0.13 ± 0.11	1.1 ± 2	1.5 ± 0.5
Type-4, Subsong n = 9	0.10 ± 0.01	35.8 ± 7.5*	18.3 ± 6.5	908 ± 159	940 ± 113	85 ± 3	5.8 ± 1.1	N.A.	3.9 ± 0.4	4.7 ± 1.0
Type-4, Plastic n = 10	0.10 ± 0.02	56.4 ± 26.8*	18.1 ± 6.1	939 ± 100	939 ± 162	84 ± 13	7.0 ± 2.6	0.016 ± 0.023	3.6 ± 1.0	4.8 ± 1.0
Interclass differences ($P < 0.01$)	2<1,3,4	1<2<4<3	1<2<3,4	3<1<2<4	3<2<4	3<1<2<4	1,3<2<4	2,4<3<1	3<1,2<4	2,3<4

Values are ± SD. Asterices indicate significant within class differences of singing versus nonsinging data ($P < 0.01$, paired t-tests). Interclass comparisons indicate significant differences between cell classes ($P < 0.01$, unpaired t-tests). Peak rate was computed as 99th percentile rate during singing. For the percent of spikes within a burst, and the number of spikes per bursts, bursts were defined as neural events exceeding 250 Hz (see METHODS). The correlation coefficient was measured to assess, the correlation of spiking activity to syllable timing on fast (~10 ms) timescales (see METHODS for detailed information on these parameters).

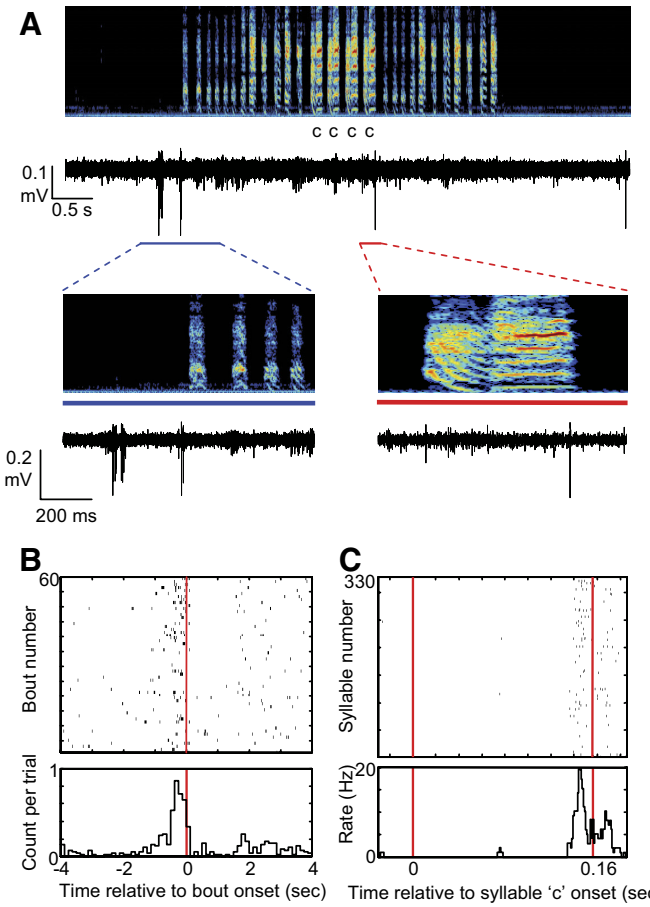

FIG. 3. Example of a type-1 neuron the activity of which was correlated with both bout onsets as well as a specific syllable. *A*: the raw voltage trace is plotted beneath the spectrogram (age dph 69). Note neuronal discharge that immediately precedes the onset of the song bout. An additional spike occurs during some renditions of syllable "c." *Bottom*: expanded views of the periods indicated by the blue line and red lines, respectively. *B*: song bout onset aligned spike raster, showing neural activity aligned to the onset of 60 consecutive bouts and the rate histogram of the raster, showing a peak in the probability of spiking that precedes bout onset. *C*: data are layed out as in *B* for neural activity aligned to 330 renditions of syllable c.

nificant variability in their firing rate across repeated trials of identified syllables (Fig. 4*F*). Trial-to-trial cross correlations coefficients computed across smoothed spike trains over repeated syllable renditions were significantly lower than in type-1 neurons (CC = 0.017 ± 0.02, Table 1) but were still significantly different from randomly shuffled spike trains in most syllables (Fig. 4*F*, Table 1, n = 10/14 syllables, 6 birds, see METHODS). In the syllable-aligned rate histograms, significant peaks in firing rate were more common than rate minima, and these modulations were distributed throughout syllables (Fig. 4*G*).

Type-3 neurons were tonically active and did not generate high-frequency bursts

Type-3 neurons were tonically active during nonsinging periods (12.3 ± 6.9 Hz, n = 29) and exhibited increased firing rates during singing (65.1 ± 19.8 Hz, $P < 0.001$, paired t-test compared with nonsinging, n = 29/29 neurons; Fig. 5). This singing-related change in firing rate occurred abruptly at song onset and offset, such that the ISI distributions and the spike

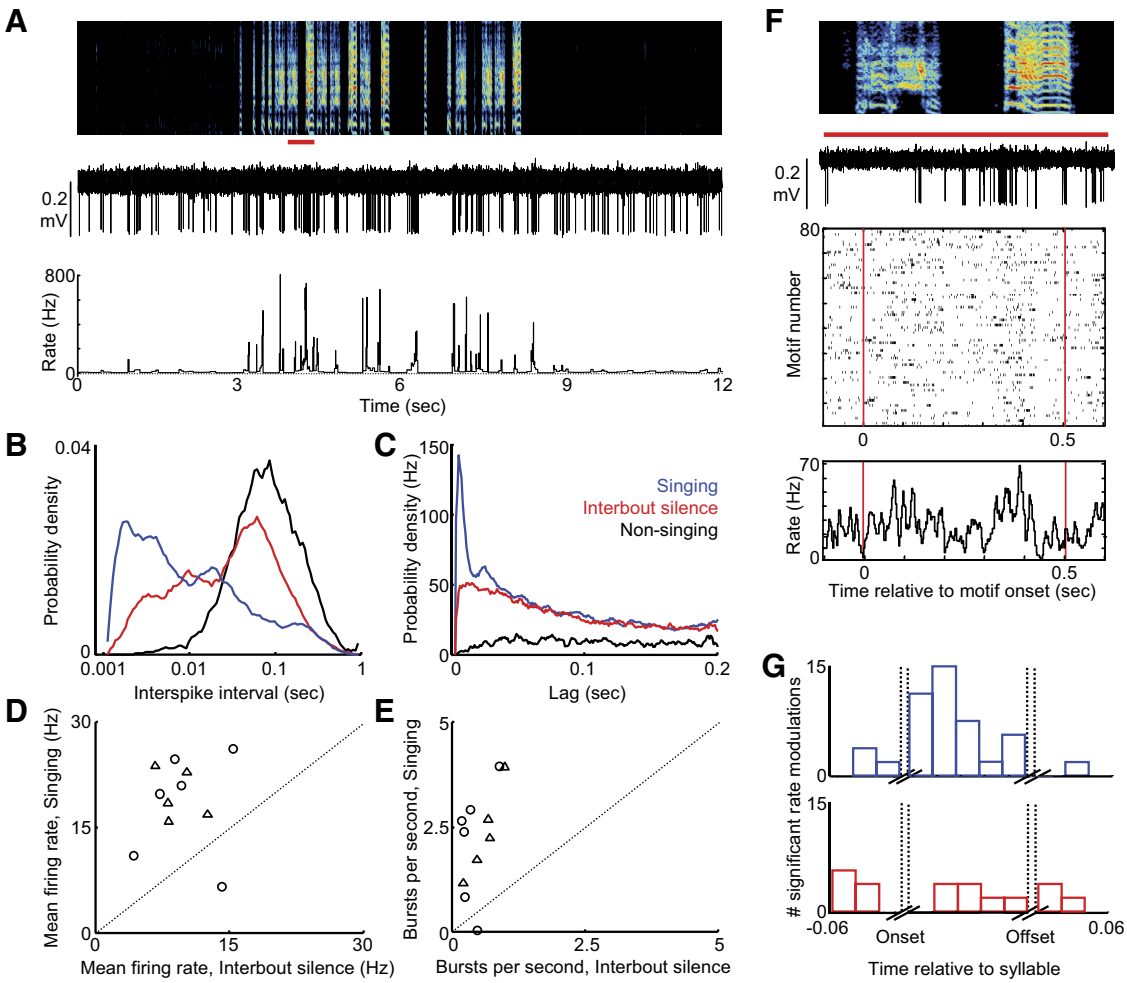

FIG. 4. Thin-spiking, type-2 neurons exhibit brief high-frequency bursts during singing. *A*: the raw voltage trace of a representative type-2 neuron and its instantaneous firing rate (see METHODS) are plotted beneath the song spectrogram (age 61 dph). *B*: interspike interval (ISI) distributions for the neuron shown in *A* during nonsinging (black), singing (blue), and interbout silent periods (red, see METHODS). *C*: spike train autocorrelation for the neuron from *A* exhibiting a narrow peak representing the brief bursts during singing. *D*: for each type-2 neuron, the mean firing rate during singing is plotted against the mean rate during interbout silence. *E*: the number of bursts per second during singing is plotted against burst incidence during interbout periods for each type-2 neuron. Triangles and circles, cells from subsong and plastic song birds, respectively. *F, top*: expanded view of a segment of the voltage waveform and spectrogram from *B* (indicated by red bar). *Middle*: spike raster showing activity of this neuron during 80 renditions of a 2-syllable motif. *Bottom*: rate histogram compiled from the raster plot. *G*: population histogram showing the distribution of significant rate peaks (blue) and rate minima (red) as a function of syllable timing (14 syllables from 6 type-2 neurons). Note that significant modulations occur throughout the syllables.

train autocorrelations during interbout and during nonsinging periods differed only slightly (Fig. 5, *B* and *C*).

In contrast to all other cell types, type-3 neurons never discharged at rates >500 Hz (peak rate = 285 ± 78 Hz, Fig. 1*F*, Table 1). During singing, type-3 neurons had ISI distributions and autocorrelograms that resembled Poisson processes with a refractory period (CV = 1.00 ± 0.2; Fig. 5, *B* and *C*). No measure of type-3 neuronal activity was different between subsong and plastic song birds (Table 1, $n = 17$ and 12 neurons from subsong and plastic song birds, respectively).

In plastic song birds, type-3 neurons spiked throughout the song (sparseness index = 0.014 ± 0.010, $n = 14$ neurons) and showed significant rate modulations that were locked to song timing (Fig. 5*F*). Rate modulations in type-3 neurons were less reproducible across syllable renditions than those of type-1 neurons but more reproducible than those of type-2 neurons (Table 1, CC = 0.13 ± 0.11, pairwise cross correlations were significant in 49/55 syllables from 14 neurons in 6 birds). Significant rate increases and decreases occurred throughout syllables, and showed no clustering around syllable onsets or offsets (Fig. 5*G*).

Type-4 neurons exhibit long, high-frequency bursts in excess of 1 kHz during singing

During nonsinging periods, type-4 neurons rarely spiked, although they occasionally generated a high-frequency burst of spikes (<0.01 burst/s, $n = 19/19$ neurons; Fig. 6). Anecdotally, the appearance of spontaneous bursting appeared to anticipate the onset of singing within the next tens of seconds (see METHODS). Bursts in type-4 neurons were robust events, often reaching rates in excess of 1 kHz (average peak rate = 955 ± 185 Hz), and consisted of an average 6.5 ± 2.1 spike/burst. In addition, type-4 neurons rarely generated single spikes—during both singing and interbout silence, nearly all spikes were part of a burst (85 ± 9% of spikes were contained in a burst, $n = 19$ neurons, Table 1). Bursting was associated with a

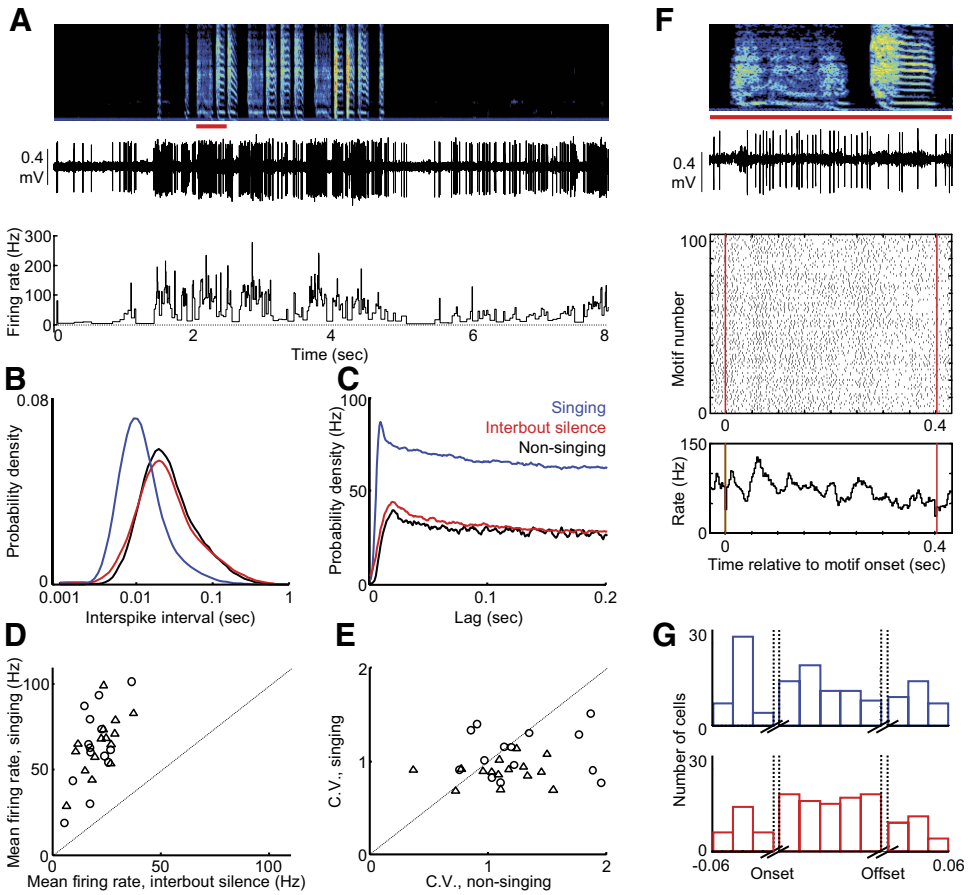

FIG. 5. Type-3 neurons are tonically active and do not generate high-frequency bursts. *A*: the raw voltage trace of a representative type-3 neuron and its instantaneous firing rate (see METHODS) are plotted beneath the song spectrogram (58-day-old bird). *B*: ISI distributions for the neuron shown in *A* during nonsinging (black), singing (blue), and interbout silent silence (red, see METHODS). *C*: spike train autocorrelation for the neuron from A. *D*: for each type-3 neuron, the mean firing rate during singing is plotted against the mean rate during interbout periods. *E*: the number of bursts per second during singing is plotted against burst incidence during interbout silence for each type-3 neuron. Triangles and circles, cells from subsong and plastic song birds, respectively. *F, top*: expanded view of the voltage and spectrogram from *A* (indicated by red bar). *Middle*: spike raster showing activity of this neuron during 100 renditions of the motif; *bottom*: the rate histogram compiled from the raster plot. *G*: population histogram showing the distribution of significant rate peaks (blue) and rate minima (red) as a function of syllable timing (54 syllables from 14 type-3 neurons). Note that significant modulations occur throughout the syllables.

single peak in the ISI distributions (Fig. 6*B*) and a broad peak in the spike train autocorrelations at short times (Fig. 6*C*).

While bursts occurred more frequently during singing than during interbout silent periods (Fig. 6, *D* and *E,* singing: 6.2 ± 2.6 burst/s interbout: 2.2 ± 0.8 burst/s, $P < 0.01$ paired *t*-test compared with interbout silence), both of these states exhibited bursting far more often than in nonsinging periods, when bursts were extremely rare (<0.01 burst/s). The statistics of bursting and of singing-related changes in activity were similar in subsong and plastic song birds (Table 1, $n = 10$ and 9 neurons from subsong and plastic song birds, respectively).

In plastic song birds, type-4 neurons spiked throughout the song (sparseness index = 0.020 ± 0.011, $n = 10$ neurons) and exhibited significant variability across repeated syllable renditions (Fig. 6*F*; CC = 0.016 ± 0.02, 17/35 syllables exhibited significant CCs compared with shuffled spike trains, see METHODS). Despite this variability, many type-4 neurons showed significant peaks and minima in the syllable-aligned rate histograms. Peaks and minima were distributed throughout syllables and not clustered at syllable onsets or offsets (Fig. 6*G*).

Salient differences in singing-related firing patterns across distinct cell types

All four cell types had distinct singing-related firing patterns that were reflected in distinct spiking statistics. Type-1 neurons fired sparsely and occasionally generated bursts, as seen in their population-average ISI distribution and spike train autocorrelation function (Fig. 7, *A* and *B,* black trace). In addition, because the firing rate within bursts was very high relative to the mean rate, the peak of the normalized spike train autocorrelation function was nearly an order of magnitude higher than that of the other cell classes (Fig. 7*B*).

On superficial examination of the spike trains, neurons in the other cell classes (types 2–4) could appear to exhibit similar singing-related firing patterns: They all discharged at low rates when the bird was not singing, and all exhibited high variable firing rates during singing. However, differences among neurons types 2–4 were immediately visible in their population-average ISI distributions and spike train autocorrelations (Fig. 7, *A*–C). For example, type-3 neurons did not burst, exhibiting flat spike train autocorrelations (Fig. 7*C*) with the longest absolute refractory period (1st percentile ISI = 3.8 ± 1.2 ms, Fig. 7*A*). Type-4 neurons, on the other hand, discharged primarily in bursts and exhibited the shortest refractory period (1st percentile ISI = 1.1 ± 0.2 ms; Fig. 7, *A*–C).

To quantify the differences in firing patterns among cell types 2–4, we examined three measures of burstiness: CV of the ISI distribution, the number of spikes per burst, and the fraction of spikes within a burst. Type-3 neurons exhibited a significantly lower CV of the ISIs during singing than other cell types, and were the least bursty (Fig. 7, *D* and *E,* Table 1). In contrast, type-4 neurons exhibited the most robust bursting by all measures. In all of these measures, type-2 neurons fell intermediate to, and partially overlapping with, type-3 and -4 neurons. Note that, despite this partial overlap, type-2 neurons were clearly distinguished from the other cell types by their narrower spike width (Fig. 1).

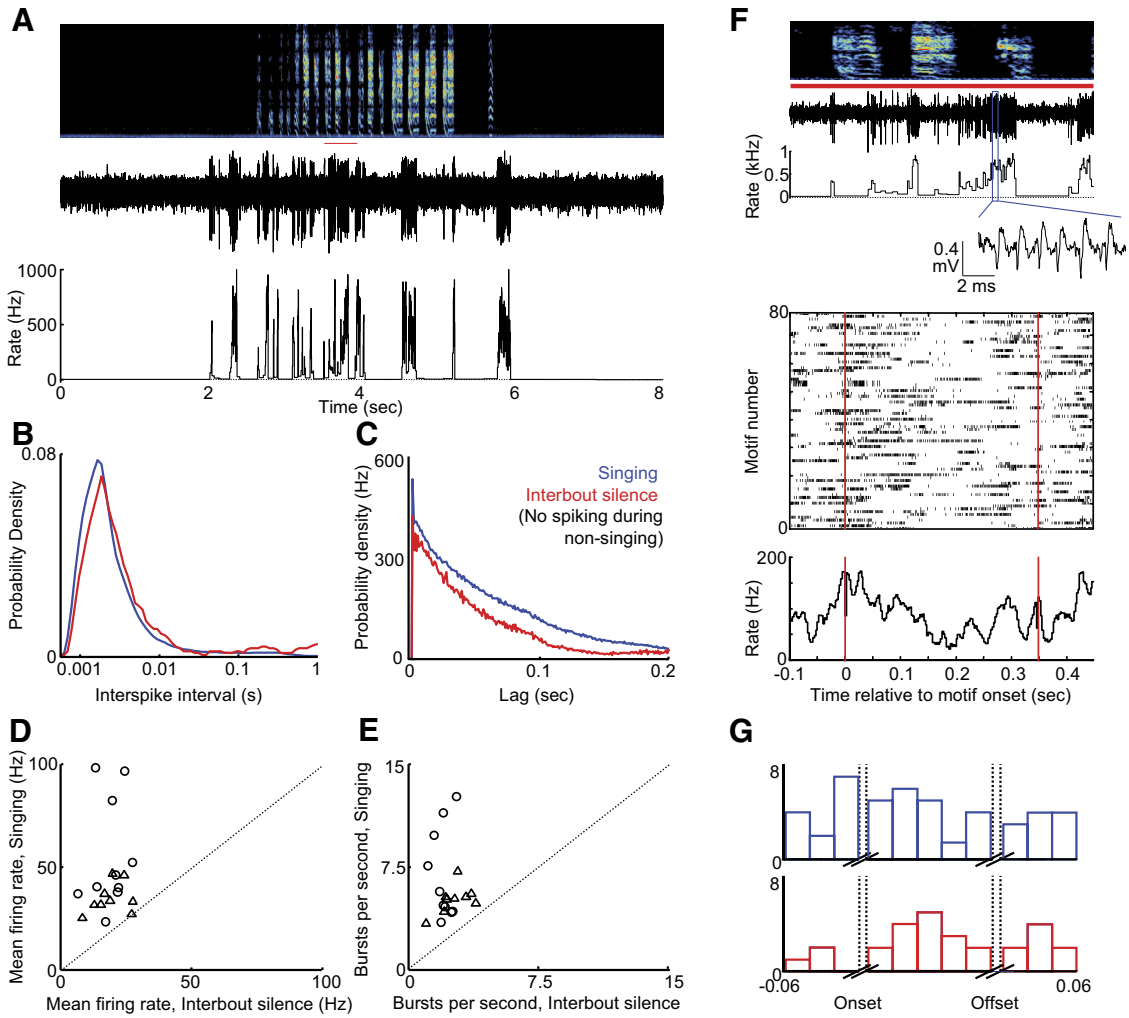

FIG. 6. Type-4 neurons exhibit broad, high-frequency bursts in excess of 1 kHz during singing. *A*: the raw voltage trace of a representative type-4 neuron and its instantaneous firing rate (see METHODS) are plotted beneath the song spectrogram (age 64 dph). *B*: ISI distributions for the neuron shown in *A* during singing (blue) and interbout silence (red, see METHODS). Type-4 neurons did not spike during nonsinging periods. *C*: spike train autocorrelation for the neuron from *A*. Note the broad peak, resulting from the long bursts of these neurons. *D*: for each type-4 neuron, the mean firing rate during singing is plotted against the mean rate during interbout periods. *E*: the number of bursts per second during singing is plotted against burst incidence during interbout periods for each type-4 neuron. Triangles and circles, cells from subsong and plastic song birds, respectively. *F, top*: expanded view of the voltage and spectrogram from *A* (indicated by red bar). *Inset*: zoom-in on a portion of a high-frequency burst. *Bottom*: spike raster indicating spiking activity of this neuron during 80 renditions of the motif, and the rate histogram compiled from the raster plot. *G*: population histogram showing the distribution of significant rate peaks (blue) and rate minima (red) as a function of syllable timing (35 syllables from 9 type-4 neurons). Note that significant modulations occur throughout the syllables.

DISCUSSION

The songbird area X is a BG nucleus specialized for singing behavior and is required for song learning (Scharff and Nottebohm 1991; Sohrabji et al. 1990). Previous studies of area X in brain slices of adult birds have identified six cell classes—two pallidal cell types and four striatal cell classes homologous to mammalian striatal neurons: MSNs, FS interneurons, cholinergic TANs, and low-threshold spiking interneurons (Farries and Perkel 2002; Farries et al. 2005). We have recorded from 185 neurons in area X in the singing bird and, based on spike waveforms and singing-related firing patterns, report six distinct cell classes. In this study, we focus on the activity of four types that exhibited low spontaneous firing rates. We hypothesize that these four cell types correspond to the four striatal cell types known to reside in area X. Because the measurement of neural activity through extracellular recording alone is insufficient to unambiguously classify neurons into distinct types, future recordings combined with juxtacellular or intracellular labeling of area X neurons will be needed confirm these hypotheses. The two high firing classes—putative pallidal neurons—were the subject of a separate study (Goldberg et al., unpublished data).

Type-1 neurons exhibit sparse temporally precise neural activity

Several features of type-1 activity lead us to hypothesize that they are the MSNs of area X. First, type-1 neurons were distinguished by their low firing rates during singing and their sparse, temporally precise relationship to song structure (Figs. 1 and 2). The vast majority of units recorded in the striatum of primates and rodents, determined to be MSNs based on in vivo intracellular labeling studies (Wilson and Groves 1981), exhibit low firing rates and a sparse, temporally precise correlation to specific stages of a behavioral sequence (Barnes et al. 2005; Hikosaka et al. 2006; Jin et al. 2009; Kimchi et al. 2009). Second, MSNs are by far the most numerous cell type in both

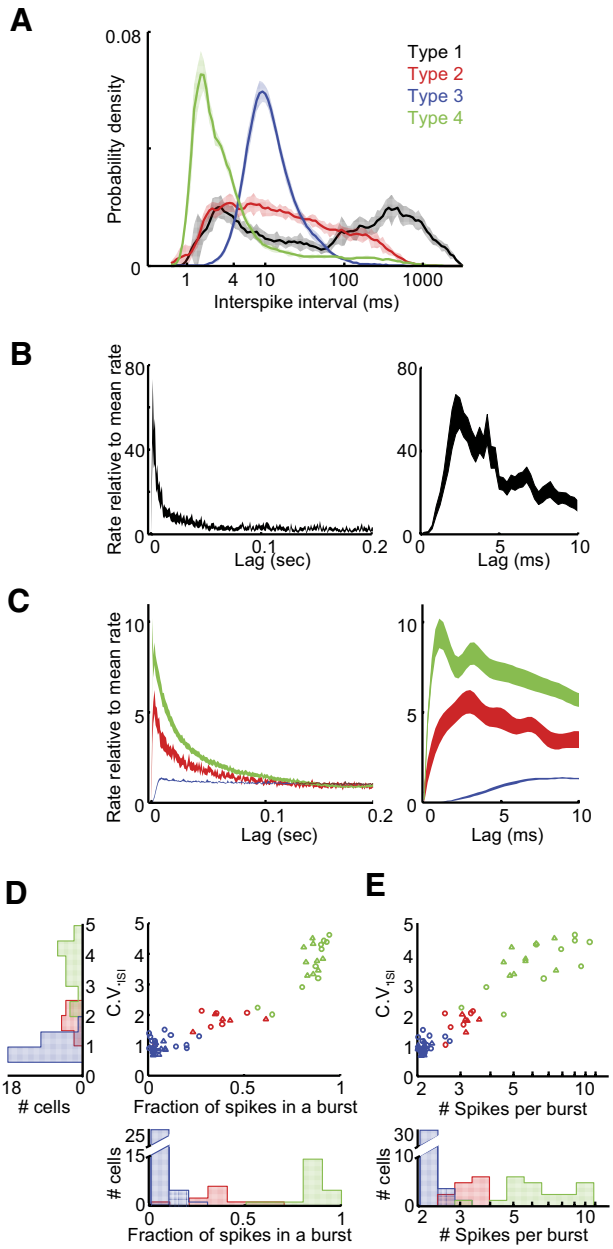

FIG. 7. Distinct bursting behavior in different cell types. *A*: population-average ISI distributions (mean ± SE) are distinct for all neuronal types. Color code as in Fig. 1. Note the 2 peaks exhibited by type-1 neurons: the peak at short intervals resulting from bursts, and the peak at long intervals resulting from their sparse firing. *B*: population-average spike train autocorrelations (mean ± SE) for type-1 neurons. *Right*: expanded view of the peak at short times. *C*: population-average spike train autocorrelations (mean ± SE) for type-2-4 neurons. Note the different vertical scale. *Right*: expanded view of the peaks at short times. Note the relatively long refractory period of type-3 neurons. *D*: for each type-2, -3 and -4 neuron, the coefficient of variation of the ISI distribution (CV_{ISI}) is plotted against the fraction of all spikes that are contained within a burst. *E*: CV vs. the average number of spikes per burst. *Left*: population histogram of CV_{ISI}; *bottom*: population histograms for data in *D* and *E*. Color code as in Fig. 1.

area X (Farries and Perkel 2002), and in the mammalian striatum (Kawaguchi et al. 1995); they were also the most frequently encountered area X neuron in our study ($n = 56/115$ neurons) despite the fact that they were likely undersampled due to their low spontaneous firing rate (Figs. 1–3). Finally, in primates, cortical neurons that project to the striatum exhibit firing patterns—including low firing rates with sparse activity temporally correlated with movement—that are remarkably similar to the MSNs they target (Crutcher and Alexander 1990; Turner and DeLong 2000). Similarly, projection neurons in the premotor cortical nucleus HVC (used as a common name) of adult and older juvenile birds discharge like type-1 neurons, exhibiting sparse bursts precisely locked to song timing (Kozhevnikov and Fee 2007). Thus the activity in both primate MSNs and in area X type-1 neurons is very similar to the activity in their cortical inputs.

However, a difference between the behavior of type-1 neurons in this study and MSNs recorded in mammals is that mammalian MSNs can exhibit significant variability in their mean firing rates with some neurons nearly silent (<0.1 Hz) and others significantly more active (~5 Hz) (Hikosaka et al. 2006; Wilson 1993). In contrast, type-1 neurons formed a homogenous group, silent outside of singing, and sparsely active during singing. This may reflect the fact that area X is entirely devoted to singing behavior—and not involved in nonsinging behaviors such as grooming, eating, or flight (Feenders et al. 2008; Nottebohm et al. 1976). In contrast, in mammals striatal circuits that serve one behavior may be spatially interwoven with those that serve another. In addition, this difference may also reflect basic interspecies differences in MSN function.

Type-2 neurons exhibited narrow spike waveforms and brief, high-frequency bursts

Several features of type-2 neurons lead us to hypothesize that they are the FS interneurons of area X. First, FS neurons were distinguished in brain slices from all other area X striatal cell classes by their narrow spike waveforms (Farries and Perkel 2002). This feature has been used to characterize mammalian striatal FS interneurons recorded in vivo, where juxtacellular labeling unambiguously identified striatal neurons with narrow spike waveforms as FS cells (Mallet et al. 2005). Second, during behavior, rodent FS interneurons exhibited constant discharge (~10 Hz) and were significantly less correlated with stages of a maze task than the putative MSNs (Berke 2008; Berke et al. 2004). Type-2 neurons were also constantly active (~8 Hz) and weakly correlated with song timing, exhibiting correlation coefficients significantly less than what was observed in type-1 neurons (Table 1). Finally, like type-2 neurons, striatal FS interneurons recorded in vivo exhibit brief high-frequency bursts that are associated with bimodality in their ISI distributions and peaks in their autocorrelograms (Fig. 4) (Berke 2008; Mallet et al. 2005; Schmitzer-Torbert and Redish 2004; Sharott et al. 2009).

Type-3 neurons were tonically active and did not generate high-frequency bursts

We hypothesize that type-3 neurons correspond to the cholinergic TANs in area X. Like TANs in the mammalian striatum, area X cholinergic neurons recorded in adult birds have large aspiny dendritic arbors, discharge spontaneously at low rates, and exhibit long spike afterhyperpolarizations (AHPs) (Farries and Perkel 2002). The long AHPs of TANS result in their having the longest absolute refractory period of all BG neuronal subtypes and prevent them from discharging at high frequencies (Kawaguchi 1993). Similarly, type-3 neurons were tonically active and had the longest absolute refractory period of all area X subtypes. Their

spike train autocorrelograms—flat with a relatively long postspike suppression (Fig. 7*D*)—resemble spike train autocorrelograms of TANs recorded in primates and rodents (Raz et al. 1996; Schmitzer-Torbert and Redish 2004).

There are several features of type-3 neurons that are not perfectly consistent with TANs recorded in mammals. First, TANS recorded extracellularly in mammals exhibit wide complex spike waveforms (Apicella et al. 1991; Crutcher and DeLong 1984; Kimura et al. 1984; Raz et al. 1996), and in vivo intracellular studies demonstrate that mammalian cholinergic TANs exhibit wider action potentials than other striatal cell types (Reynolds et al. 2004; Wilson et al. 1990). In contrast, type-3 neurons did not exhibit unusually wide or complex spike waveforms (Fig. 1). Although diverging from the mammalian data, this finding is not inconsistent with intracellular recordings in area X brain slice, where many cholinergic neurons did not exhibit significantly wider spikes than other cell types (Farries and Perkel 2002). Another difference is that the firing rates of type-3 neurons during singing (~60 Hz) were significantly higher than what is typically observed in TANS recorded in behaving mammals (~10–20 Hz) (Apicella et al. 1991; Kimura et al. 1984). While these differences could reflect interspecies variations in TAN physiology, we note that the behaviorally-related firing rates (either peak or average) of all area X neurons were higher than their mammalian counterparts by about the same factor of 3–4 (Goldberg et al. 2010).

Type-4 neurons discharged primarily in long, high-frequency bursts

The identification of type-4 neurons is made difficult by the lack of a clearly homologous firing pattern recorded in the BG of behaving mammals. To our knowledge, there are no reports of striatal neurons recorded in behaving animals that discharge almost exclusively in high-frequency bursts as we found for type-4 neurons. However, one striatal cell type—low-threshold spiking interneurons—identified in songbird area X and mammalian striatal slice recordings, exhibit pronounced calcium spikes that drive high-frequency "rebound bursts" at the offset of hyperpolarizing current injections (Farries and Perkel 2002; Kawaguchi 1993). Some area X LTS interneurons discharged spontaneously in slice with nearly all of their spikes discharging within bursts (Farries and Perkel 2002). In addition, putative LTS neurons recorded in the anesthetized rodent fire almost exclusively in bursts that reached the highest rates of all striatal cell classes (Sharott et al. 2009). Thus one possibility is that type-4 neurons correspond to the LTS interneurons in area X. An alternative possibility, however, is that type-4 neurons correspond to another cell type not yet discovered in area X slice recordings, for example low-frequency bursting units that have been reported in the primate pallidus (DeLong 1971).

Firing rate modulations of area X neurons were correlated with song temporal structure

It has been hypothesized that the BGs of both mammals and songbirds implement trial-and-error learning (Andalman and Fee 2009; Doya 2000, 1999; Kao et al. 2005; Ölveczky et al.

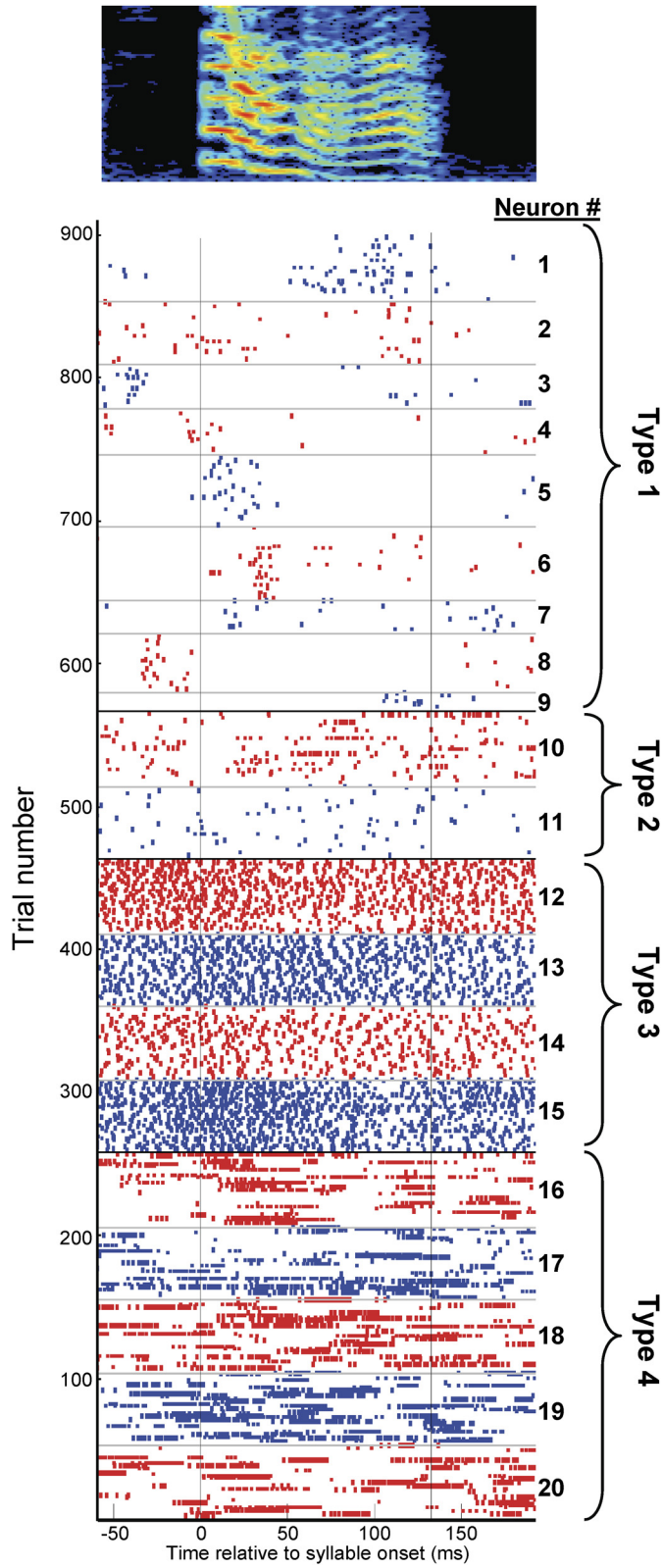

FIG. 8. Singing-related activity of 20 area X neurons recorded during a single syllable in a single bird, aged 51–55 dph. Each row in the raster shows the singing-related spikes during 1 rendition of the syllable. Alternating red and blue colors indicate different area X neurons with the hypothesized subtype indicated at right. Neurons type 1–4 are, respectively, putative medium spiny neurons, fast spikers, TANs, and low-threshold spikers.

2005; Tumer and Brainard 2007). In songbirds, lesions or inactivation of LMAN, the output of the AFP (Fig. 1), eliminate variability in juvenile song (Bottjer et al. 1984; Ölveczky et al. 2005), whereas lesions to area X result in abnormal acoustic structure and persistent variability as if exploration occurs without appropriate evaluation (Scharff and Nottebohm 1991). Thus it has been hypothesized that area X generates "error signals" that direct song learning (Doupe et al. 2004; Doya 1999), but the nature of area X signals have remained unknown.

Here we report that, just as striatal neurons exhibit activity temporally correlated with distinct stages of a behavioral task (Aosaki et al. 1994; Barnes et al. 2005; Berke 2008), all area X cell classes exhibited temporal correlations to song on fast (~10 ms) time scales. To illustrate the population activity of area X neurons during singing, we aligned the spike trains of twenty neurons recorded in a single bird to the onset of a single syllable (Fig. 8). First, we selected nine type-1 neurons that spiked during this syllable; other type-1 neurons ($n = 6$) were silent during this syllable but spiked during other syllables. Note that the type-1 neurons, putative MSNs, spiked sparsely, and preferentially at a specific time within the syllable, but different neurons recorded in the same bird spiked at different times in the song (Figs. 2 and 8). Type-2 neurons, putative FS interneurons, spiked irregularly throughout the syllable, occasionally discharging in brief, high-frequency bursts (Figs. 4 and 8). Type-3 neurons, putative TANS, were tonically active throughout the syllable, and produced regular spike trains without bursts (Figs. 5 and 8). Finally, type-4 neurons, putative LTS interneurons, discharged mostly in long, high-frequency bursts, the timing of which was weakly correlated with the song (Figs. 6 and 8). Notably, all cell types exhibited correlations to song timing that, as a population, were distributed throughout the song.

These data suggest that the population of neurons in area X can encode timing information continuously during singing. Such distributed coding of time during a motor sequence is useful in solving the temporal credit assignment problem and has been explicitly predicted in models where BG circuits implement reinforcement learning (Montague et al. 1996). In addition, it has recently been demonstrated that the output of the AFP generates an error signal that biases vocal output, in real time, to improve performance (Andalman and Fee 2009). If the correlations to song timing we have observed in area X play a role in generating this bias, the continuous encoding of time during singing would allow such premotor bias to be implemented at any point in the song.

Where do these correlations to song timing originate? Area X has two glutamatergic inputs. HVC neurons that project to area X exhibit brief bursts precisely time-locked to the song (Kozhevnikov and Fee 2007). In contrast, LMAN neurons spike variably with weaker correlations to song timing (Kao et al. 2005; Leonardo 2004; Ölveczky et al. 2005). Thus we hypothesize that HVC plays the major role in driving timing information in area X neurons and, in particular, the type-1 neurons that strongly resemble HVC neurons in their firing patterns.

Because area X and LMAN are interconnected within a loop, it is difficult to isolate the origins of variability within the circuit. It is noteworthy that the putative MSNs (type-1) at the input layer of area X, exhibit activity that is significantly more correlated to song timing than other cell types, including pallidal neurons that represent area X output (Goldberg et al. 2010). This could suggest that variability emerges within the striato-pallidal circuit. Another possibility, however, is that while type-1 neurons are driven primarily by inputs from HVC, other area X cell types that exhibit more spiking variability could be driven primarily by inputs from LMAN. Indeed direct inputs to area X pallidal neurons from both HVC and LMAN have been demonstrated in brain slice recordings (Farries et al. 2005) and inferred in vivo (Leblois et al. 2009), and functionally resemble the "hyperdirect" pathway in mammals (Nambu et al. 2002). Thus additional experiments such as recordings of area X neurons during LMAN inactivation are needed to resolve the issue of where variability originates in basal-ganglia thalamocortical circuits.

Summary

Our results represent the first characterization of the singing-related neural activities of multiple cell types in a BG nucleus required for song learning and provide a testable framework for the classification of striatal neurons in the singing bird. Given the highly conserved nature of vertebrate BG circuits (Reiner 2009), future studies aimed at understanding how area X cell classes interact during behavior and what role their signals may play in learning are likely to elucidate fundamental principles of BG function.

ACKNOWLEDGMENTS

We thank Dmitry Aronov and Aaron Andalman for helfpful suggestions regarding data analysis.

GRANTS

Funding to M. S. Fee was provided by National Institute of Deafness and Other Communication Disorder Grant R01DC-009183 and to J. H. Goldberg by the Damon Runyon Research Foundation and Charles King Trust Postdoctoral Fellowships.

REFERENCES

Andalman AS, Fee MS. A basal ganglia-forebrain circuit in the songbird biases motor output to avoid vocal errors. *Proc Natl Acad Sci USA* 106: 12518–12523, 2009.

Aosaki T, Kimura M, Graybiel AM. Temporal and spatial characteristics of tonically active neurons of the primate's striatum. *J Neurophysiol* 73: 1234–1252, 1995.

Aosaki T, Tsubokawa H, Ishida A, Watanabe K, Graybiel AM, Kimura M. Responses of tonically active neurons in the primate's striatum undergo systematic changes during behavioral sensorimotor conditioning. *J Neurosci* 14: 3969–3984, 1994.

Apicella P. Leading tonically active neurons of the striatum from reward detection to context recognition. *Trends Neurosci* 30: 299–306, 2007.

Apicella P, Scarnati E, Schultz W. Tonically discharging neurons of monkey striatum respond to preparatory and rewarding stimuli. *Exp Brain Res* 84: 672–675, 1991.

Aronov D, Andalman AS, Fee MS. A specialized forebrain circuit for vocal babbling in the juvenile songbird. *Science* 320: 630–634, 2008.

Bar-Gad I, Heimer G, Ritov Y, Bergman H. Functional correlations between neighboring neurons in the primate globus pallidus are weak or nonexistent. *J Neurosci* 23: 4012–4016, 2003.

Barnes TD, Kubota Y, Hu D, Jin DZ, Graybiel AM. Activity of striatal neurons reflects dynamic encoding and recoding of procedural memories. *Nature* 437: 1158–1161, 2005.

Berke JD. Uncoordinated firing rate changes of striatal fast-spiking interneurons during behavioral task performance. *J Neurosci* 28: 10075–10080, 2008.

Berke JD, Okatan M, Skurski J, Eichenbaum HB. Oscillatory entrainment of striatal neurons in freely moving rats. *Neuron* 43: 883–896, 2004.

Bottjer SW, Miesner EA, Arnold AP. Forebrain lesions disrupt development but not maintenance of song in passerine birds. *Science* 224: 901–903, 1984.

Crutcher MD, Alexander GE. Movement-related neuronal activity selectively coding either direction or muscle pattern in three motor areas of the monkey. *J Neurophysiol* 64: 151–163, 1990.

Crutcher MD, DeLong MR. Single cell studies of the primate putamen. II. Relations to direction of movement and pattern of muscular activity. *Exp Brain Res* 53: 244–258, 1984.

DeLong MR. Activity of pallidal neurons during movement. *J Neurophysiol* 34: 414–427, 1971.

DeLong MR. Activity of basal ganglia neurons during movement. *Brain Res* 40: 127–135, 1972.

Doupe AJ, Solis MM, Kimpo R, Boettiger CA. Cellular, circuit, and synaptic mechanisms in song learning. *Ann NY Acad Sci* 1016: 495–523, 2004.

Doya K. What are the computations of the cerebellum, the basal ganglia and the cerebral cortex? *Neural Netw* 12: 961–974, 1999.

Doya K. Complementary roles of basal ganglia and cerebellum in learning and motor control. *Curr Opin Neurobiol* 10: 732–739, 2000.

Farries MA, Ding L, Perkel DJ. Evidence for "direct" and "indirect" pathways through the song system basal ganglia. *J Comp Neurol* 484: 93–104, 2005.

Farries MA, Perkel DJ. A telencephalic nucleus essential for song learning contains neurons with physiological characteristics of both striatum and globus pallidus. *J Neurosci* 22: 3776–3787, 2002.

Fee MS, Leonardo A. Miniature motorized microdrive and commutator system for chronic neural recording in small animals. *J Neurosci Methods* 112: 83–94, 2001.

Feenders G, Liedvogel M, Rivas M, Zapka M, Horita H, Hara E, Wada K, Mouritsen H, Jarvis ED. Molecular mapping of movement-associated areas in the avian brain: a motor theory for vocal learning origin. *PLoS One* 3: e1768, 2008.

Field D. What is the goal of sensory coding? *Neural Comput* 6: 559–601, 1994.

Goldberg J, Avital A, Bergman H, Free MS. Singing-related neural activity distinguishes two putative pallidal cell types in the songbird basal ganglia: Comparison to the primate internal and external pallidal segments. *J Neurosci.* 2010, In press.

Graybiel AM. Habits, rituals, and the evaluative brain. *Annu Rev Neurosci* 31: 359–387, 2008.

Hahnloser RH, Kozhevnikov AA, Fee MS. An ultra-sparse code underlies the generation of neural sequences in a songbird. *Nature* 419: 65–70, 2002.

Hikosaka O, Nakamura K, Nakahara H. Basal ganglia orient eyes to reward. *J Neurophysiol* 95: 567–584, 2006.

Hikosaka O, Wurtz RH. The basal ganglia. *Rev Oculomot Res* 3: 257–281, 1989.

Jin DZ, Fujii N, Graybiel AM. Neural representation of time in cortico-basal ganglia circuits. *Proc Natl Acad Sci USA* 106: 19156–19161, 2009.

Johnstone S, Rolls ET. Delay, discriminatory, and modality specific neurons in striatum and pallidum during short-term memory tasks. *Brain Res* 522: 147–151, 1990.

Kao MH, Doupe AJ, Brainard MS. Contributions of an avian basal ganglia-forebrain circuit to real-time modulation of song. *Nature* 433: 638–643, 2005.

Kao MH, Wright BD, Doupe AJ. Neurons in a forebrain nucleus required for vocal plasticity rapidly switch between precise firing and variable bursting depending on social context. *J Neurosci* 28: 13232–13247, 2008.

Kawaguchi Y. Physiological, morphological, and histochemical characterization of three classes of interneurons in rat neostriatum. *J Neurosci* 13: 4908–4923, 1993.

Kawaguchi Y, Wilson CJ, Augood SJ, Emson PC. Striatal interneurones: chemical, physiological and morphological characterization. *Trends Neurosci* 18: 527–535, 1995.

Kimchi EY, Torregrossa MM, Taylor JR, Laubach M. Neuronal correlates of instrumental learning in the dorsal striatum. *J Neurophysiol* 102: 475–489, 2009.

Kimura M, Rajkowski J, Evarts E. Tonically discharging putamen neurons exhibit set-dependent responses. *Proc Natl Acad Sci USA* 81: 4998–5001, 1984.

Kozhevnikov AA, Fee MS. Singing-related activity of identified HVC neurons in the zebra finch. *J Neurophysiol* 97: 4271–4283, 2007.

Kreitzer AC. Physiology and pharmacology of striatal neurons. *Annu Rev Neurosci* 32: 127–147, 2009.

Kubota Y, Kawaguchi Y. Dependence of GABAergic synaptic areas on the interneuron type and target size. *J Neurosci* 20: 375–386, 2000.

Kubota Y, Mikawa S, Kawaguchi Y. Neostriatal GABAergic interneurons contain NOS, calretinin or parvalbumin. *Neuroreport* 5: 205–208, 1993.

Leblois A, Bodor AL, Person AL, Perkel DJ. Millisecond timescale disinhibition mediates fast information transmission through an avian basal ganglia loop. *J Neurosci* 29: 15420–15433, 2009.

Lehky SR, Sejnowski TJ, Desimone R. Selectivity and sparseness in the responses of striate complex cells. *Vision Res* 45: 57–73, 2005.

Lenz S, Perney TM, Qin Y, Robbins E, Chesselet MF. GABA-ergic interneurons of the striatum express the Shaw-like potassium channel Kv3.1. *Synapse* 18: 55–66, 1994.

Leonardo A. Experimental test of the birdsong error-correction model. *Proc Natl Acad Sci USA* 101: 16935–16940, 2004.

Mallet N, Le Moine C, Charpier S, Gonon F. Feedforward inhibition of projection neurons by fast-spiking GABA interneurons in the rat striatum in vivo. *J Neurosci* 25: 3857–3869, 2005.

Mink JW. The basal ganglia: focused selection and inhibition of competing motor programs. *Prog Neurobiol* 50: 381–425, 1996.

Montague PR, Dayan P, Sejnowski TJ. A framework for mesencephalic dopamine systems based on predictive Hebbian learning. *J Neurosci* 16: 1936–1947, 1996.

Morris G, Arkadir D, Nevet A, Vaadia E, Bergman H. Coincident but distinct messages of midbrain dopamine and striatal tonically active neurons. *Neuron* 43: 133–143, 2004.

Nambu A, Tokuno H, Takada M. Functional significance of the cortico-subthalamo-pallidal "hyperdirect" pathway. *Neurosci Res* 43: 111–117, 2002.

Nottebohm F, Stokes TM, Leonard CM. Central control of song in the canary, Serinus canarius. *J Comp Neurol* 165: 457–486, 1976.

Ölveczky BP, Andalman AS, Fee MS. Vocal experimentation in the juvenile songbird requires a basal ganglia circuit. *PLoS Biol* 3: e153, 2005.

Packard MG, Knowlton BJ. Learning and memory functions of the basal ganglia. *Annu Rev Neurosci* 25: 563–593, 2002.

Plenz D, Kitai ST. Up and down states in striatal medium spiny neurons simultaneously recorded with spontaneous activity in fast-spiking interneurons studied in cortex-striatum-substantia nigra organotypic cultures. *J Neurosci* 18: 266–283, 1998.

Raz A, Feingold A, Zelanskaya V, Vaadia E, Bergman H. Neuronal synchronization of tonically active neurons in the striatum of normal and parkinsonian primates. *J Neurophysiol* 76: 2083–2088, 1996.

Reiner A. You cannot have a vertebrate brain without a basal ganglia. In: *The Basal Ganglia IX*. New York: Springer, 2009, p. 3–24.

Reynolds JN, Hyland BI, Wickens JR. Modulation of an afterhyperpolarization by the substantia nigra induces pauses in the tonic firing of striatal cholinergic interneurons. *J Neurosci* 24: 9870–9877, 2004.

Scharff C, Nottebohm F. A comparative study of the behavioral deficits following lesions of various parts of the zebra finch song system: implications for vocal learning. *J Neurosci* 11: 2896–2913, 1991.

Schmitzer-Torbert N, Redish AD. Neuronal activity in the rodent dorsal striatum in sequential navigation: separation of spatial and reward responses on the multiple T task. *J Neurophysiol* 91: 2259–2272, 2004.

Sharott A, Moll CK, Engler G, Denker M, Grun S, Engel AK. Different subtypes of striatal neurons are selectively modulated by cortical oscillations. *J Neurosci* 29: 4571–4585, 2009.

Sohrabji F, Nordeen EJ, Nordeen KW. Selective impairment of song learning following lesions of a forebrain nucleus in the juvenile zebra finch. *Behav Neural Biol* 53: 51–63, 1990.

Tchernichovski O, Nottebohm F, Ho CE, Pesaran B, Mitra PP. A procedure for an automated measurement of song similarity. *Anim Behav* 59: 1167–1176, 2000.

Tolhurst DJ, Smyth D, Thompson ID. The sparseness of neuronal responses in ferret primary visual cortex. *J Neurosci* 29: 2355–2370, 2009.

Tumer EC, Brainard MS. Performance variability enables adaptive plasticity of "crystallized" adult birdsong. *Nature* 450: 1240–1244, 2007.

Turner RS, DeLong MR. Corticostriatal activity in primary motor cortex of the macaque. *J Neurosci* 20: 7096–7108, 2000.

Wilson CJ. The generation of natural firing patterns in neostriatal neurons. *Prog Brain Res* 99: 277–297, 1993.

Wilson CJ, Chang HT, Kitai ST. Firing patterns and synaptic potentials of identified giant aspiny interneurons in the rat neostriatum. *J Neurosci* 10: 508–519, 1990.

Wilson CJ, Groves PM. Spontaneous firing patterns of identified spiny neurons in the rat neostriatum. *Brain Res* 220: 67–80, 1981.

Zhou FM, Wilson CJ, Dani JA. Cholinergic interneuron characteristics and nicotinic properties in the striatum. *J Neurobiol* 53: 590–605, 2002.